

# Analyst

Accepted Manuscript



This is an *Accepted Manuscript*, which has been through the Royal Society of Chemistry peer review process and has been accepted for publication.

*Accepted Manuscripts* are published online shortly after acceptance, before technical editing, formatting and proof reading. Using this free service, authors can make their results available to the community, in citable form, before we publish the edited article. We will replace this *Accepted Manuscript* with the edited and formatted *Advance Article* as soon as it is available.

You can find more information about *Accepted Manuscripts* in the [Information for Authors](#).

Please note that technical editing may introduce minor changes to the text and/or graphics, which may alter content. The journal's standard [Terms & Conditions](#) and the [Ethical guidelines](#) still apply. In no event shall the Royal Society of Chemistry be held responsible for any errors or omissions in this *Accepted Manuscript* or any consequences arising from the use of any information it contains.

# ***In situ* molecular imaging of hydrated biofilm in a microfluidic reactor by ToF-SIMS**

Xin Hua,<sup>ab</sup> Xiao-Ying Yu,<sup>\*a</sup> Zhaoying Wang,<sup>c</sup> Li Yang,<sup>c</sup> Bingwen Liu,<sup>a</sup> Zihua Zhu,<sup>c</sup> Abigail E. Tucker,<sup>d</sup> William B. Chrisler,<sup>d</sup> Eric A. Hill,<sup>d</sup> Theva Thevuthasan,<sup>c</sup> Yuehe Lin,<sup>e</sup> Songqin Liu<sup>b</sup> and Matthew J. Marshall<sup>\*d</sup>

One Sentence Significance

**A novel microfluidic reactor for biofilm growth was constructed to enable *in situ* chemical imaging of hydrated biofilms using ToF-SIMS.**

## COMMUNICATION

## *In situ* molecular imaging of hydrated biofilm in a microfluidic reactor by ToF-SIMS

Cite this: DOI: 10.1039/x0xx00000x

Received 7th December 2013  
Accepted 00th xxxxxxxx 2013

DOI: 10.1039/c3an00000x

www.rsc.org/analyst

Xin Hua,<sup>ab</sup> Xiao-Ying Yu,<sup>\*a</sup> Zhaoying Wang,<sup>c</sup> Li Yang,<sup>c</sup> Bingwen Liu,<sup>a</sup> Zihua Zhu,<sup>c</sup> Abigail E. Tucker,<sup>d</sup> William B. Chrisler,<sup>d</sup> Eric A. Hill,<sup>d</sup> Theva Thevuthasan,<sup>c</sup> Yuehe Lin,<sup>e</sup> Songqin Liu<sup>b</sup> and Matthew J. Marshall<sup>\*d</sup>

**A novel microfluidic reactor for biofilm growth and in situ characterization using time-of-flight secondary ion mass spectrometry (ToF-SIMS) was constructed to enable two-dimensional chemical imaging of hydrated biofilms. We demonstrate the detection of characteristic fatty acid fragments from microfluidic reactor-grown biofilms and illustrate advantages of hydrated-state ToF-SIMS imaging.**

This paper reports a unique approach of molecular imaging of biofilms in their native environments using time-of-flight secondary ion mass spectrometry (ToF-SIMS) to address potentially the grand challenge of complex interfacial dynamics in biogeochemistry.<sup>1</sup> Biofilm is grown on a silicon nitride (SiN) membrane window in a recently developed microfluidic flow cell as a single channel flow reactor.<sup>2-4</sup> Continuous imaging of complex liquid samples can be performed with high precision and sensitivity using this technique.<sup>5,6</sup> Direct probing of the biofilm occurs *in situ* within a windowless detection area of 2  $\mu\text{m}$  in diameter as soon as the hole is drilled through by the SIMS primary ion beam.

One of the most important processes in nature involves bacteria forming surface attached microbial communities or biofilms.<sup>7</sup> Biofilms possess a complex structure made of a highly-hydrated milieu containing bacterial cells and self-generated extracellular polymeric substances (EPS).<sup>8</sup>

<sup>a</sup>Fundamental and Computer Sciences, Pacific Northwest National Laboratory (PNNL), Richland, WA 99352. Email: xiaoying.yu@pnnl.gov; Phone: 1-509-372-4524; Fax: 1-509-372-6168

<sup>b</sup>School of Chemistry and Chemical Engineering, Southeast University, Nanjing, Jiangsu Province, P. R. China, 211189.

<sup>c</sup>W. R. Wiley Environmental Molecular Science Laboratory, PNNL, Richland, WA 99352.

<sup>d</sup>Biological Sciences Division, PNNL, Richland, WA 99352. Email: matthew.marshall@pnnl.gov; Phone: 1-509-371-6964; Fax: 1-509-371-6955

<sup>e</sup>Physical Sciences Division, PNNL, Richland, WA 99352.

† Electronic supplementary information (ESI) available: See DOI: 10.1039/c000000x/

Flow cells have been developed to make microscopic observations of biofilm growth possible.<sup>9</sup> Stain-based approaches, such as confocal laser scanning microscopy (CLSM), have been used to monitor hydrated biofilm development and physiology.<sup>10</sup> Previous work has shown that biofilms develop metabolic and chemical heterogeneities that affect overall biological activities as biofilms respond to environmental microenvironments at the individual cell level.<sup>11-13</sup> However, prerequisite chemical modifications required for vacuum based imaging of biofilm microenvironments, such as the removal of water, can cause drastic changes to EPS integrity and biofilm morphology.<sup>14</sup> *In situ* molecular imaging tools are necessary in understanding how the spatial heterogeneity and structural difference affect the microbial community activities in an unperturbed, hydrated state.<sup>15</sup>

ToF-SIMS is a unique surface analytical tool that provides molecular information (*e.g.*, mass spectra) and image mapping with a lateral resolution of  $\sim 0.2 \mu\text{m}$ . It has been used increasingly in characterizing biological and soft materials.<sup>16</sup> However, most known applications are limited to solid samples because of the challenge to detect liquids with high volatility in a vacuum chamber. We have recently developed a portable microfluidic interface to address this challenge and direct imaging of liquid surfaces using ToF-SIMS is now possible. This capability was demonstrated in the high vacuum mode in scanning electron microscopy (SEM)<sup>2</sup> and comparison between this approach and environmental SEM (ESEM) was discussed elsewhere.<sup>3, 17</sup> Previous design consideration and validation<sup>3</sup> demonstrated that temperature drop across the aperture is only a few K, thus freezing is not an issue. Beam damage is overcome by either renewing the detection surface and passing liquid continuously through the aperture via an electroosmotic pump<sup>3</sup> or using the diffusivity of liquid itself within the microfluidic channel aggravated by evaporation at the aperture in vacuum. This liquid ToF-SIMS application enables direct probing of the anisotropic and heterogeneous interfacial region that is relevant to biofilm attachment and adhesion to surfaces.

We report here the first *in situ* hydrated, molecular imaging results of a biofilm grown in a single channel microfluidic flow reactor using ToF-SIMS. Comparisons of hydrated biofilms grown

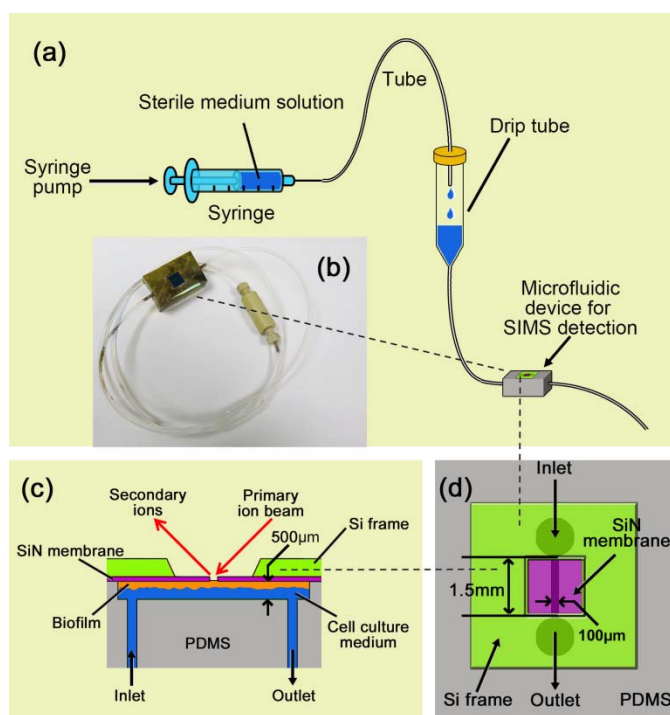


**Fig. 1** Schematic of the single-channel growth microfluidic reactor and ToF-SIMS detection including (a) setup of the biofilm growth experiment, (b) a photo of the device used for biofilm growth; (c) schematic showing the cross perspective of the grown biofilm during ToF-SIMS probing; and (d) a top view perspective of the device during biofilm growth.

in the microfluidic reactor were directly made with dehydrated biofilm samples and an uninoculated liquid medium solution. ToF-SIMS  $m/z$  spectra and 2D images revealed differences in chemical compositions and spatial distributions. Furthermore, principal component analysis (PCA) results show clear distinctions among these samples. This approach provides a novel pathway to study *in situ* biofilm physiology at the molecular level and understand complex environmental processes as biofilms interact with surfaces across multiple domains (*e.g.*, from molecular to mesoscale).

Detailed device fabrication and interface assembly were described in our earlier papers.<sup>2,3</sup> Soft photolithography was used to make the microfluidic channel on a polydimethylsiloxane (PDMS) block.<sup>17</sup> To reduce the possibility of clogging during the biofilm growth, the microfluidic channel dimension was chosen to be 100  $\mu\text{m}$  wide by 500  $\mu\text{m}$  deep. Two holes were punched at the two ends of the microchannel to form inlet and outlet for bacteria inoculation and delivery of growth medium. See the ESI† for more details.

ToF-SIMS imaging and detection was conducted using a ToF-SIMS V spectrometer (IONTOF GmbH, Münster, Germany). Detailed SIMS conditions were given in the ESI†. PCA was achieved using PLS\_Toolbox 6.7.1 (Eigenvector Research, Inc., Manson, WA, USA) in Matlab 2012(a) (MathWorks Inc., Natick, MA, USA). Data were preprocessed by autoscaling prior to PCA analysis.

The experimental setup for biofilm growth was depicted in Fig. 1.

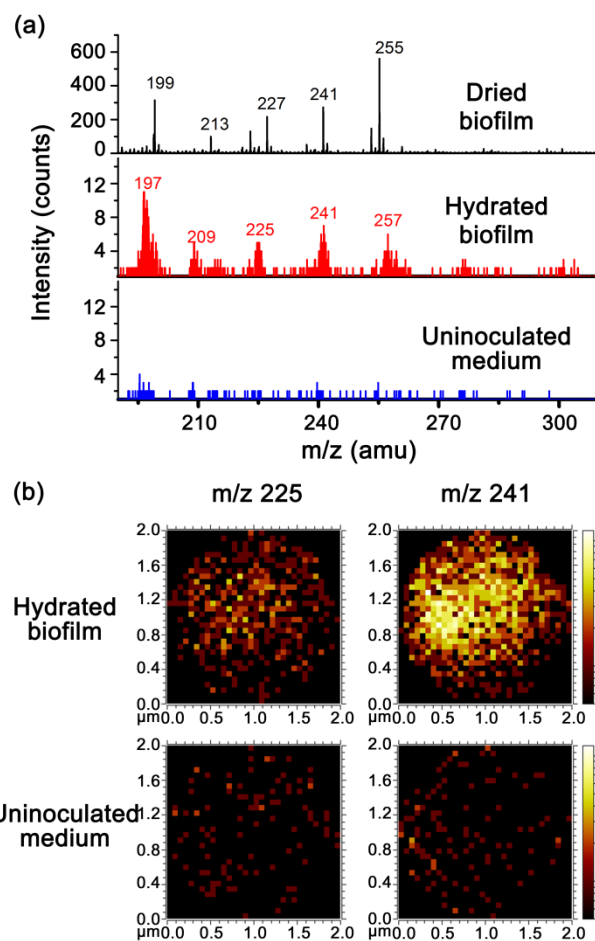


**Fig. 2** (a) Representative ToF-SIMS  $m/z$  spectra of dried *Shewanella* sp. biofilm deposited on clean Si wafer, hydrated biofilm, and uninoculated medium solution and (b) 2D images of  $m/z$  225 ( $\text{C}_{14}$  FA) and  $m/z$  241 ( $\text{C}_{15}$  FA) fragments obtained from the hydrated biofilm and uninoculated medium samples. The false-colour scale shown on the right of (b) indicates relative SIMS signal intensity from high (white/yellow) to low (black/red).

The microfluidic device was placed on a small platform and the PTFE tubing portion was taped to the platform to prevent it from moving around. A transparent plastic cover was used to keep dust off. A needle was inserted into the inlet tubing and this assembly was connected to a custom-made manifold that allows fresh medium delivery. To harvest the microfluidic reactor for ToF-SIMS imaging, the reactor was stopped and immediately sealed prior to attaching to the ToF-SIMS stage for analysis within 1 hr. of harvesting.

Our previous studies have demonstrated the feasibility of a microfluidic reactor as an analytical tool for SIMS analysis of aqueous samples.<sup>2-6</sup> Here, we showed that our microfluidic reactor was robust enough to support SIMS drilling at multiple points across the channel dimensions without compromising the integrity of SiN membrane and underlying aqueous samples under vacuum. This facilitated obtaining biological replicates within a sample and provided the possibility to study biofilm spatial differences across the microfluidic channel.

ToF-SIMS provides molecular recognition for organic or biological molecules. Effort has been made to study biofilms using

ToF-SIMS recently using either dried<sup>18</sup> or cryosection samples.<sup>19</sup> [M-H]<sup>-</sup> peaks (representing quasi molecular ions typically formed from loss of a hydrogen) are commonly observed molecular ion peaks in the negative mode of ToF-SIMS spectra.<sup>20</sup> The ToF-SIMS negative  $m/z$  spectrum showing characteristic fragments of dried biofilms was depicted in Fig. 2(a).

2D images of characteristic fatty acids (FA) fragments obtained from the hydrated biofilms grown in a microfluidic reactor were depicted in Fig. 2(b). In the hydrated biofilms grown in the microfluidic reactor, SIMS revealed several peaks between  $m/z$  200-300 amu. No discernible SIMS peaks were found in the uninoculated medium (Fig. 2(a)), which demonstrated that the peaks observed in the hydrated biofilm samples were specific to biofilm growth. SIMS also revealed characteristic peaks of FA fragments such as  $m/z$  199, 213, 227, 241 and 255 in the dried biofilm samples. These  $m/z$  FA fragments were similar to peaks in the hydrated biofilm and partially in accordance with a previous report for dried *Shewanella* cells on hematite.<sup>21</sup> Results presented here were obtained from mass range of smaller than 300 amu, because the primary aim was to compare with the dried biofilm samples to ascertain the validity of the new approach. With the increased  $m/z$  scanning range, it is likely other peaks of interest to characteristic EPS fractions and diatoms may be observed as reported in recent studies.<sup>18, 19</sup>

Assignments of the dried biofilm peaks were displayed in Table S1†, in which  $m/z$  199 was attributed to  $C_{12}H_{23}O_2^-$  (lauric acid),  $m/z$  213 to  $C_{13}H_{25}O_2^-$  (tridecyl acid),  $m/z$  227 to  $C_{14}H_{27}O_2^-$  (myristic acid),  $m/z$  241 to  $C_{15}H_{29}O_2^-$  (pentadecyl acid) and  $m/z$  255 to  $C_{16}H_{31}O_2^-$  (palmitic acid). Comparison between our work and the LIPID MAPS Structure Database (LMSD, <http://www.lipidmaps.org/data/structure/>) showed slight shifts potentially due to sample uniformity and instrument responses in an experiment (see Table S1†).<sup>22</sup>

The spectra of the hydrated biofilm sample have lower counts mainly due to (1) poor geometry around the aperture area reduces collection efficiency of secondary ions, and (2) the experimental settings might not be fully optimized. An interesting observation is that the spectra of dry film and hydrated film look similar, however, some peaks were shifted (e.g., in Fig 2(a),  $m/z$  197, 209, 225, 257 in hydrated films vs. 199, 213, 227, 255 in dried samples). More than one biofilm samples were analysed and similar phenomena occurred. The spectrum of the uninoculated medium solution showed no characteristics peaks, unlike the hydrated biofilm sample. This confirms that the characteristic peaks indeed came from the hydrated biofilm. Currently, we do not have an explanation for the peak shift between dried and hydrated films. However, this observation suggests that the surface chemical components may change during the biofilm drying, and *in situ* characterization is necessary.

High spatial resolution is preferable to observe liquid surface over the windowless portion of the flow cell after the SiN membrane was drilled through by the primary ion beam. Secondary ion images with a  $10 \times 10 \mu m^2$  area were obtained from microfluidic reactors containing hydrated biofilms or uninoculated medium using the imaging mode after punching through the SiN membrane (Fig. S3†).

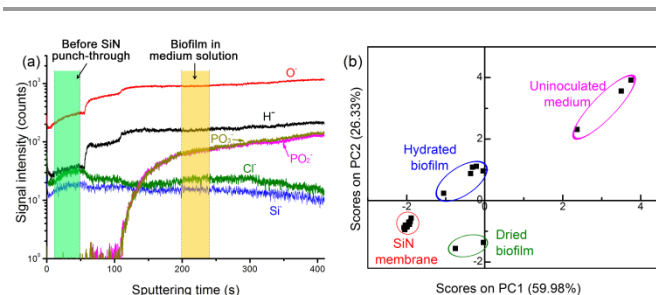


Fig 3 (a) ToF-SIMS depth profiles of several key components of a biofilm sample grown in the microfluidic reactor. The shaded areas (e.g., green indicates before SiN punch-through and orange biofilm in medium solution) give examples of selected data segments for PCA analysis. (b) PCA results showing distinctions among hydrated biofilm, uninoculated medium solution, dried biofilm samples from 200-240 s, and SiN membrane data from 10-50 s in (a).

The overlay of  $Si^-$  and  $PO_2^-$  fragments clearly demonstrated that the SiN membrane was drilled through and displayed the shape and size (i.e.,  $\sim 2 \mu m$  in diameter) of the aperture (Fig. S3†).

False-colour SIMS maps of qualitative spatial distributions and concentration gradients for observed peaks are shown in Fig. 2(b). The 2D images show representative biofilm fragments in the liquid surface ( $m/z$  227 and  $m/z$  241) corresponding to  $C_{14}$  and  $C_{15}$  straight chain FA fragments. In both images, a concentration gradient across the hydrated region might be indicative of chemical spatial differences at the sample site. Furthermore, visual comparisons between the concentration gradients for hydrated biofilm and uninoculated medium samples illustrated that the characteristic SIMS fragments of biofilm were distinguishable. This demonstrated the feasibility of our approach for label free, *in situ* imaging of microbial biofilms.

The ToF-SIMS primary ion beam was used to drill the aperture and simultaneously excite the secondary ion beam of the fragments and consequently acquire real-time composition information of a sample in the depth profiling mode. A depth profile was obtained as shown in Fig. 3a, which provides time- and space-resolved depiction of the SiN substrate, biofilm (resolved from the substrate attached interface towards the fluid interface), and the biofilm suspended in medium solution past the biofilm/fluid interface (see shaded areas corresponding to different sputtering time in the depth profile and ESI†). Fig. 3a illustrated the signal changes of six ion fragments:  $H^-$ ,  $O^-$ ,  $Si^-$ ,  $Cl^-$ ,  $PO_2^-$  and  $PO_3^-$ . Sharp intensity rises for  $H^-$  and  $O^-$  coupled with decrease of  $Si^-$  at  $\sim 52$  s indicated the beginning of SiN membrane punch-through. Another sudden increase of  $PO_2^-$  and  $PO_3^-$  at  $\sim 110$  s suggested that the SiN membrane was thoroughly punched through and the liquid surface was being detected. Along the depth profiling temporal series, 52-110 s and 110-150 s are considered to be the transition period, where two small bumps were seen. After  $\sim 150$  s, signals of  $H^-$  and  $O^-$  flattened out and the increase of  $PO_2^-$  and  $PO_3^-$  signals slowed down, indicating that a relatively stable and renewable liquid surface formed in the aperture.

Normally, the information depth for static ToF-SIMS is estimated to be a few nm according to reported SIMS emission depth measurements.<sup>3, 23</sup> However, the interface is very dynamic in this approach. As described in Fig. S4†, high current density was used (i.e.,  $>4 \times 10^{16}$  ions/cm<sup>2</sup>), and

1 SiN/biofilm erosion occurred continuously. Also, in a liquid  
2 system, ion species of interest may diffuse from the adjacent  
3 biofilm/medium solution interface or the bulk to the aperture  
4 area (e.g.,  $10^{-9}$ – $10^{-6}$  m)<sup>24</sup>. Furthermore, the aqueous solution  
5 surface is self-renewable due to evaporation and capillary effect  
6 within the microchannel. Therefore, the SIMS spectra shown  
7 here contain information not only from the SiN/biofilm  
8 interface (a few nm thick), but also from the medium solution  
9 (up to a few microns) and the aperture side wall (SiN/biofilm).

10 PCA was employed to evaluate the intrinsic similarities and  
11 discriminations among samples. Integrations of characteristic peaks  
12 from ToF-SIMS spectra during 40 s before and after the transition  
13 period were exported for PCA analysis, which were defined as  
14 “before SiN punch-through” and “biofilm in medium solution” and  
15 depicted in Fig. 3a. For the dried biofilm samples, high mass  
16 resolution spectra were collected within a scanning area of (100×100  
17  $\mu\text{m}^2$ ). The composition was homogeneous according to the signal  
18 intensity-time relationship shown in Fig. S2†. The spectra between  
19 various segments (e.g., 200–240 s) were pretreated by autoscaling  
20 instead of mean centring. Mean centring is useful to ensure the first  
21 principal component (PC1) describes the direction of maximum  
22 variance. It is sensitive to peaks with higher intensity (i.e., H<sup>+</sup>, O<sup>-</sup>)  
23 while contributions from peaks with lower intensity (i.e.,  $m/z$  227,  
24 241) were almost omitted. Autoscaling results in data having a  
25 standard deviation of one; and the analysis is then based on  
26 correlations instead of covariances as in mean centring.

27 Fig. 3(b) shows the PCA score plot that revealed four distinct  
28 clusters of SIMS data representing: the SiN membrane, the hydrated  
29 biofilm after punching through the SiN membrane, the uninoculated  
30 medium solution after the aperture was drilled through, and dried  
31 biofilm sample on a Si wafer. These data clusters were compelling  
32 evidence that liquid biofilm was indeed observed by ToF-SIMS,  
33 showing differences in composition among hydrated biofilm  
34 samples, dried biofilm samples, and uninoculated controls. Two  
35 principal components (PC) seem to be sufficient, as the sum of PC1  
36 and PC2 represent about 87% of all signals. The similarities  
37 observed between the hydrated and dried samples in the PC1 scores  
38 indicated that there was a common biological component between  
39 these samples. Likewise, the similarities between the hydrated  
40 biofilm and uninoculated medium solution in the PC2 scores  
41 exemplify the liquid nature of these samples. Clearly, PCA analysis  
42 of SIMS data confirmed that hydrated microfluidic reactor samples  
43 represent an important advance for *in situ* imaging of biofilms.

44 ToF-SIMS imaging results demonstrated molecular recognition  
45 for label-free organic and biological molecules enabled via a unique  
46 microfluidic reactor. Cluster ion sources have seen rapid  
47 development in the past decade resulting in  $\text{Bi}_n^+$ ,  $\text{C}_{60}^{1-2+}$  and  $\text{Ar}_n^{+16, 25}$   
48 ion beams that may provide better detection limits compared to the  
49 25 keV  $\text{Bi}^+$  ion beam used in this study.

50 We demonstrated that the innovated microfluidic device can be  
51 used for controlled biofilm cultivation and as a microreactor for *in*  
52 *situ* hydrated, molecular imaging by ToF-SIMS. Our microreactor  
53 was amiable to monitoring biofilm growth in real-time using CLSM;  
54 and ToF-SIMS was subsequently used to obtain images of the same  
55 biofilm using different modes. First, depth profiles of the biofilm  
56 were used to show drill-through of the SiN membrane and the

membrane-attached biofilm. Once the SiN membrane was removed,  
high spatial resolution  $m/z$  spectra of the biofilm were acquired.  
Characteristic FA fragments of biofilm were observed in hydrated  
samples and compared with those from dried biofilm samples using  
PCA. These analyses confirmed the microfluidic reactor as a unique  
approach for correlated biofilm growth and *in situ* molecular  
imaging. Current research is being conducted to study soluble EPS  
using the approach described here and further ascertain the  
differences or similarities between EPS and intact hydrated biofilm.  
Most importantly, this new technique provides the much sought  
opportunity to follow, in real-time and space, the hydrated state  
dynamics of biofilm attachment, growth, and dissociation dynamics  
with high resolution chemical mapping. This enables new  
opportunities to study biofilms in its native state without  
dehydration, cryogenic freezing or staining, which are currently  
needed for using vacuum based characterization techniques.

## Author contributions

The manuscript was written through contributions of all authors. All authors have given approval to the final version of the manuscript.

## Notes

The authors declare no competing financial interests.

## Acknowledgements

We are grateful to the Pacific Northwest National Laboratory (PNNL) Chemical Imaging Initiative-Laboratory Directed Research and Development (CII-LDRD) fund and the Use at Facility Funds (UAFF) for support in the design and construction of the microfluidic reactor. Biofilm studies were funded by a U.S. DOE Office of Science Early Career Research Award (Project No. 60385) and instrument time was provided through an Environmental Molecular Sciences Laboratory (EMSL) Science Themed Proposal. A US patent application (14/050,144) including the particular application of biofilm growth and molecular imaging using the microfluidic flow reactor described in this work was filed. PNNL is operated by Battelle for the DOE under Contract DE-AC05-76RL01830.

## References

1. J. K. Fredrickson, M. F. Romine, A. S. Beliaev, et al., *Nat Rev Micro*, 2008, 6, 592-603.
2. L. Yang, X.-Y. Yu, Z. Zhu, M. J. Iedema and J. P. Cowin, *Lab Chip*, 2011, 11, 2481-2484.
3. L. Yang, Y. X.-Y., Z. H. Zhu, T. Thevuthasan and J. P. Cowin, *J. Vac. Sci. Technol. A* 2011, 29, article no. 061101.
4. X.-Y. Yu, L. Yang, J. Cowin, M. Iedema and Z. Zhu, *USA Pat.*, 8,555,710, 2011.
5. L. Yang, Z. Zhu, X.-Y. Yu, S. Thevuthasan and J. P. Cowin, *Analytical Methods*, 2013, 5, 2515-2522.
6. L. Yang, Z. Zhu, X.-Y. Yu, E. Rodek, L. Saraf, T. Thevuthasan and J. P. Cowin, *Surface Interface Analysis*, 2013, doi: 10.1002/sia5252.
7. G. O'Toole, H. B. Kaplan and R. Kolter, *Annu Rev Microbiol*, 2000, 54, 49-79.

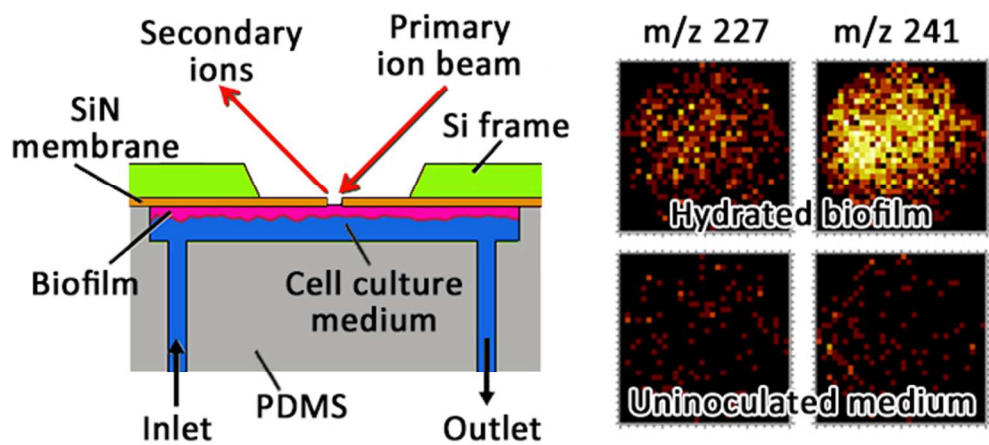
## Analyst

- 1 8. H. C. Flemming and J. Wingender, *Nat. Rev. Microbiol.*, 2010, 8, 623-
- 2 633.
- 3 9. A. J. McBain, in *Advances in Applied Microbiology*, eds. I. L. Allen, S.
- 4 Sima and M. G. Geoffrey, Academic Press, 2009, vol. Volume 69, pp.
- 5 99-132.
- 6 10. B. B. Christensen, C. Sternberg, J. B. Andersen, R. J. Palmer Jr, A.
- 7 Toftgaard Nielsen, M. Givskov and S. Molin, in *Methods in*
- 8 *Enzymology*, ed. J. D. Ron, Academic Press, 1999, vol. Volume 310, pp.
- 9 20-42.
- 10 11. J. T. Babauta, H. D. Nguyen, T. D. Harrington, R. Renslow and H.
- 11 Beyenal, *Biotechnol. Bioeng.*, 2012, 109, 2651-2662.
- 12 12. J. S. McLean, P. D. Majors, C. L. Reardon, C. L. Bilskis, S. B. Reed, M.
- 13 F. Romine and J. K. Fredrickson, *J. Microbiol. Methods*, 2008, 74, 47-
- 14 56.
- 15 13. A. E. Franks, K. P. Nevin, R. H. Glaven and D. R. Lovley, *ISME J*,
- 16 2010, 4, 509-519.
- 17 14. A. C. Dohnalkova, M. J. Marshall, B. W. Arey, K. H. Williams, E. C.
- 18 Buck and J. K. Fredrickson, *Appl. Environ. Microbiol.*, 2011, 77, 1254-
- 19 1262.
- 20 15. L. Yang, Y. Hu, Y. Liu, J. Zhang, J. Ulstrup and S. Molin, *Environ.*
- 21 *Microbiol.*, 2011, 13, 1705-1717.
- 22 16. N. Winograd, *Anal. Chem.*, 2005, 77, 142A-149A.
- 23 17. X.-Y. Yu, B. Liu and L. Yang, *Microfluid Nanofluid*, 2013, 15, 725-744.
- 24 18. J. F. C. de Brouwer, K. E. Cooksey, B. Wigglesworth-Cooksey, M. J.
- 25 Staal, L. J. Stal and R. Avci, *J. Microbiol. Methods*, 2006, 65, 562-572.
- 26 19. T. Leefmann, C. Heim, A. Kryvenda, S. Siljeström, P. Sjövall and V.
- 27 Thiel, *Organic Geochemistry*, 2013, 57, 23-33.
- 28 20. A. Benninghoven, in *ToF-SIMS: Surface Analysis By Mass*
- 29 *Spcectrometry*, ed. J. C. V. a. D. Briggs, 1st edn., 2001, pp. 41-72.
- 30 21. J. C. Ingram, W. F. Bauer, R. M. Lehman, S. P. O'Connell and A. D.
- 31 Shaw, *J. Microbiol. Methods*, 2003, 53, 295-307.
- 32 22. J. L. S. Lee, I. S. Gilmore, I. W. Fletcher and M. P. Seah, *Applied*
- 33 *Surface Science*, 2008, 255, 1560-1563.
- 34 23. B. Liu, X.-Y. Yu, Z. Zhu, X. Hua, L. Yang and Z. Wang, *Lab Chip*,
- 35 2014, doi: 10.1039/C3LC50971K.
- 36 24. A. J. Bard and F. R. Fan, *Faraday Discuss.*, 1992, 94, 1-22.
- 37 25. S. Kayser, D. Rading, R. Moellers, F. Kollmer and E. Niehuis, *Surface*
- 38 *and Interface Analysis*, 2013, 45, 131-133.
- 39
- 40
- 41
- 42

**Key words**

Hydrated biofilm, ToF-SIMS, molecular imaging, microfluidic reactor

1  
2  
3  
4  
5  
6  
7  
8  
9  
10  
11  
12  
13  
14  
15  
16  
17  
18  
19  
20  
21  
22  
23  
24  
25  
26  
27  
28  
29  
30  
31  
32  
33  
34  
35  
36  
37  
38  
39  
40  
41  
42  
43  
44  
45  
46  
47  
48  
49  
50  
51  
52  
53  
54  
55  
56  
57  
58  
59  
60



58x27mm (300 x 300 DPI)